ORIGINAL ARTICLE

https://doi.org/10.5125/jkaoms.2022.48.4.207
pISSN 2234-7550 · eISSN 2234-5930

# Investigation of the prevalence and main features of skull-base anomalies and characteristics of the sphenoid sinus using cone-beam computed tomography

Aslıhan Akbulut[1], Oğuzhan Demirel[2,3], Kaan Orhan[4,5]

[1]*Department of Dentomaxillofacial Radiology, Faculty of Dentistry, İstanbul Medipol University, İstanbul,*
[2]*Mehmet Tanrıkulu Health Services Vocational School,* [3]*Department of Dentomaxillofacial Radiology, Faculty of Dentistry, Bolu Abant İzzet Baysal University, Bolu,* [4]*Department of Dentomaxillofacial Radiology, Faculty of Dentistry, Ankara University, Ankara,*
[5]*Ankara University Medical Design Application and Research Center (MEDITAM), Ankara, Turkey*

**Abstract** (J Korean Assoc Oral Maxillofac Surg 2022;48:207-218)

**Objectives:** This study aimed to define the prevalence and characteristics of skull base anomalies and the features of sphenoid sinus pneumatization (SSP).

**Materials and Methods:** Five hundred cone-beam computed tomography scans were evaluated retrospectively for the presence of fossa navicularis magna (FNM), canalis basilaris medianus (CBM), sphenoid emissary foramen (SEF), and/or Onodi cells (OC). Patterns of the SSP and sphenoid sinus mucosa dimensions (SSMD) were also recorded.

**Results:** The prevalence of FNM, CBM, SEF, and OC was 26.0%, 22.4%, 47.4%, and 18.4%, respectively. Two hundred sixty-two (52.4%) sellar-type SSP were defined, followed by post-sellar 191 (38.2%), pre-sellar 31 (6.2%), and conchal 16 (3.2%) types. The frequency of SSMD less than 1 mm, 1-3 mm, and greater than 3 mm was 40.6%, 38.4%, and 21.0%, respectively. An SEF was detected more frequently in females, while SSMD greater than 3 mm was more frequent in males. An FNM was more prevalent in the 18-29 and 30-39 age groups and SEF was significantly less frequent in patients over 60 years of age compared to other age groups. A sinus mucosa larger than 3 mm was more common in the younger than 18 year group. The frequency of post-sellar-type pneumatization was lower in patients younger than 18 years.

**Conclusion:** Skull-base anomalies are common and may be detected incidentally during imaging procedures. The sphenoid sinus, its variations, and pneumatization patterns should also be taken into consideration in imaging procedures performed for various purposes.

**Key words:** Fossa navicularis magna, Canalis basilaris medianus, Sphenoid emissary foramen, Onodi cell, Sphenoid sinus

*[paper submitted 2022. 3. 21 / accepted 2022. 6. 14]*

## I. Introduction

The skull base is an important anatomical part of the body that acts as a border between intracranial and extracranial anatomical structures and provides a connection with several foramina and canals. The base of the skull can be divided into three portions, the anterior, middle, and posterior skull base. The posterior part of the skull base is formed mainly by the occipital bone and parts of the temporal and sphenoid bones. The middle portion of the skull base is mostly formed by the sphenoid bone and the temporal bone anterior to the petrous ridge[1]. The clivus is formed by the basal portion of the occipital bone (basiocciput) and the body of the sphenoid bone (basisphenoid)[1,2].

Another anatomical structure that lies in the middle of the skull base is the sphenoid sinus, which is associated with several vital structures such as the foramen rotundum, vidian canal, carotid canal, and pituitary gland[3].

Many previous studies have reported anatomical variations of the above-mentioned structures. Variations of the bony structures of the skull base, such as the canalis basilaris medianus (CBM), fossa navicularis magna (FNM), sphenoid emissary foramen (SEF), and of the pneumatization pattern

***Oğuzhan Demirel***
*Department of Dentomaxillofacial Radiology, Faculty of Dentistry, Bolu Abant İzzet Baysal University, Gölköy, 14030 Bolu, Turkey*
*TEL: +90-533-2370104*
*E-mail: dtoguzhandemirel@gmail.com*
*ORCID: https://orcid.org/0000-0002-4756-6496*

of the sphenoid sinus have been discussed extensively in the literature[2,4-12].

A FNM can be described as a notch-like bony defect with well-defined margins on the inferior surface of the clivus[13-15].

A CBM is a relatively rare anomaly of the basiocciput, in which a well-defined channel is present on the intracranial surface of the basiocciput. A CBM is classified primarily according to its completeness and location as bifurcation, inferior, superior, channel type, inferior recess, and superior recess[5].

A SEF is a small-sized and common anatomical variation of the middle skull base, located in the greater wing of the sphenoid bone, anterior and medial to the foramen ovale. An SEF contains a small vein connecting the cavernous sinus with the pterygoid venous plexus[16].

Onodi cells (OC) are the most posterior ethmoid air cells extending into the sphenoid sinus and are important for their proximity to vital structures and also for their influence on endoscopic sinus surgery and endonasal surgical procedures[11,17].

Sphenoid sinus pneumatization (SSP) is generally classified according to the relative location of air-filled zones with respect to the sella turcica as seen on sagittal sections as follows: conchal, pre-sellar, sellar, and post-sellar. Conchal-type pneumatization is non-pneumatization or a small pneumatization anterior to the anterior wall of the sella, while the pre-sellar type refers to pneumatization of the sphenoid sinus anterior to the anterior edge of the sella turcica. Sellar-type pneumatization can be defined as pneumatization not extending beyond the posterior wall of the sella turcica. The post-sellar type, as the name indicates, is pneumatization of the sphenoid sinus extending beyond the posterior wall of the sella[3,9].

Cone-beam computed tomography (CBCT), with its wide range of use, availability, low radiation dose, and capability of providing high-resolution images of hard tissues, is becoming a more popular option in the field of skull imaging.

This study aimed to investigate the prevalence and characteristics of skull-base anomalies and to evaluate their relationship with age and sex using CBCT. An additional aim was to assess the anomalies and pneumatization of the sphenoid sinuses and their possible correlations with skull-base anomalies.

## II. Materials and Methods

Ethical approval of the study was obtained from the ethics committee of İstanbul Medipol University, Clinical Research Ethics Committee (No. 10840098-772.02-E.34484).

### 1. Patient selection

The study included CBCT scans of 500 patients who were admitted to Oral and Maxillofacial Radiology Clinic of İstanbul Medipol University between 2012 and 2020 for various procedures, such as implant planning, pre-surgical assessment of impacted teeth, orthognathic surgery, and cyst and tumor evaluation.

Patients with a history of trauma to and/or surgery of the head and neck region, neurologic diseases, syndromes affecting the craniofacial region, and diseases affecting bone metabolism were excluded. In addition, images with artifacts (metal artifacts, motion artifacts, etc.) that could adversely affect the definition and measurement of the anomalies and pathologies were excluded.

The age and sexes of the patients were recorded. Patients were classified according to age as follows: Group 1 <18 years; Group 2, 18-29 years; Group 3, 30-39 years; Group 4, 40-49 years; Group 5, 50-59 years; and Group 6, ≥60 years.

### 2. CBCT image acquisition and image analyses

All CBCT scans were obtained using an iCAT Model 17-19 imaging system (Imaging Sciences International, Hatfield, PA, USA) with a single 360° rotation and a voxel size of 0.3 mm with the following exposure parameters: 4.8 seconds, 5.0 mA, 120 kV, and 9 to 13 mm×16 mm field of view. Acquired CBCT data were transferred to Invivo 5 ver 5.2 Anatomage dental imaging software (San Jose, CA, USA) for image analysis and measurements. All image analyses and measurements were made by the same observer who had at least 10 years of experience performing CBCT scans.

Sagittal reconstructions were used to identify the presence or absence of a FNM. A FNM was identified as a well-defined bony depression area on the inferior part of the clivus. The dimensions of an FNM were measured in the sagittal (length and depth measurements) and axial (width measurements) planes. The length of an FNM was determined on sagittal sections as the distance between the uppermost point where the depression started and the lowermost point where the depression ended. The depth of an FNM was measured as the distance from the deepest point of the depression to the line that connected the uppermost and lowermost points of the depression. On axial sections, the width of an FNM was

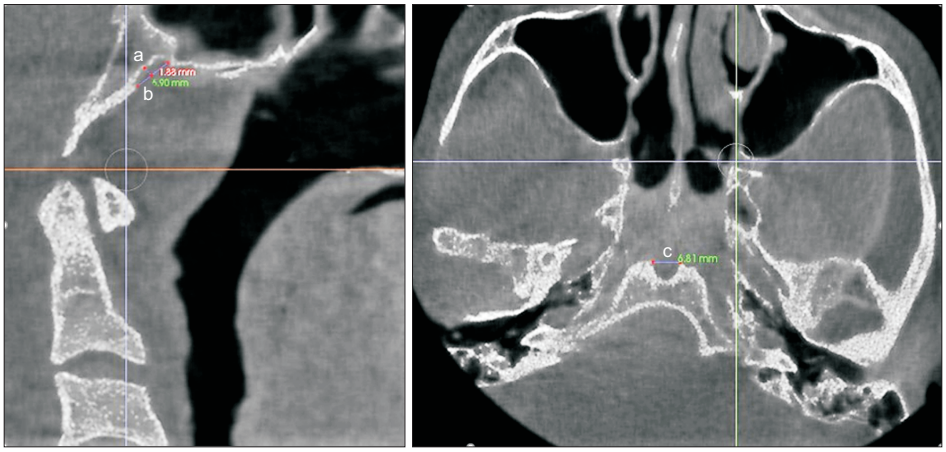


**Fig. 1.** Fossa navicularis magna and measurements (a: depth, b: length, c: width).
*Aslıhan Akbulut et al: Investigation of the prevalence and main features of skull-base anomalies and characteristics of the sphenoid sinus using cone-beam computed tomography. J Korean Assoc Oral Maxillofac Surg 2022*

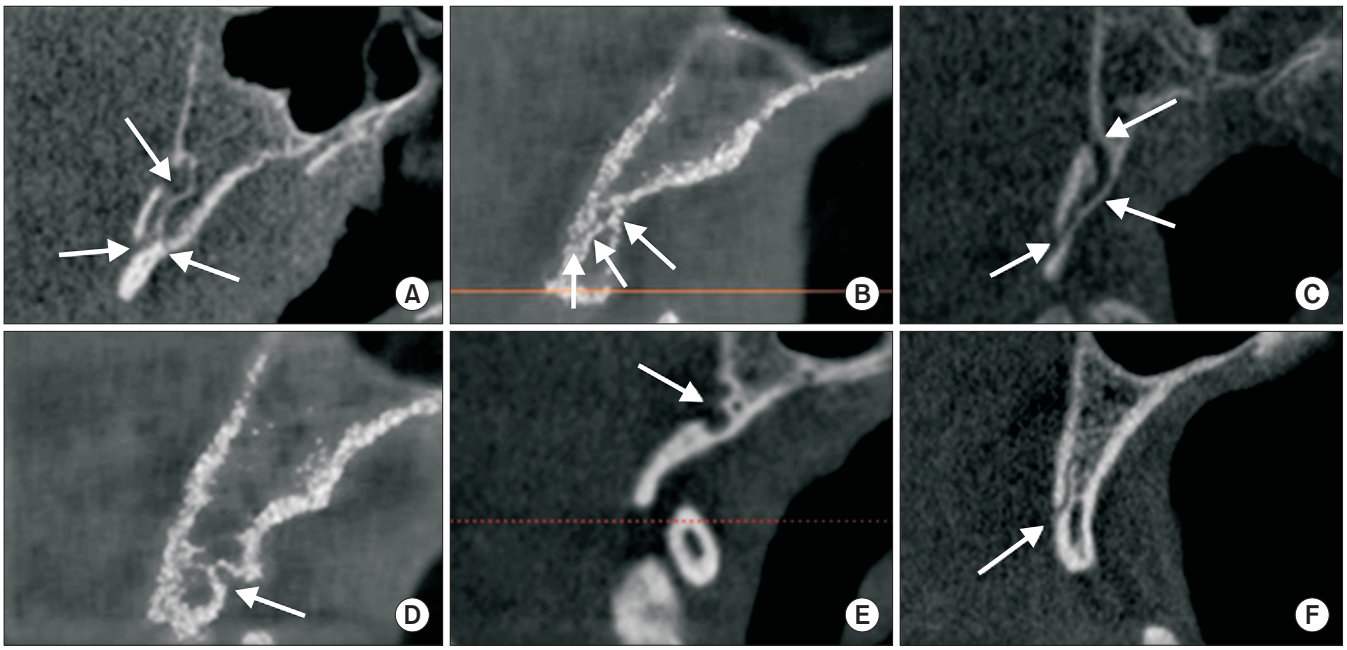


**Fig. 2.** Types of canalis basilaris medianus (arrows). A. Bifurcation. B. Inferior. C. Superior. D. Inferior recess. E. Superior recess. F. Channel type.
*Aslıhan Akbulut et al: Investigation of the prevalence and main features of skull-base anomalies and characteristics of the sphenoid sinus using cone-beam computed tomography. J Korean Assoc Oral Maxillofac Surg 2022*

measured as the distance between the lateral borders of the depression.(Fig. 1)

CBM was identified as a well-defined, corticated, transclival osseous defect located in the basiocciput of the clivus. The CBMs were classified into six sub-groups (bifurcation, inferior, superior, inferior recess, superior recess, channel-type) on sagittal sections.(Fig. 2)

A SEF was identified as a round or oval-shaped structure with sclerotic borders and a radiolucent center, visible on at least two consecutive sections. Laterality (unilateral, bilateral), shape (round, oval, irregular), type (Type 1, diameter less than 0.5 mm; Type 2, diameter between 0.5 mm and 1 mm; or Type 3, diameter greater than 1 mm) of the foramen were recorded. Measurements were made to define the diameter of the foramen and the distance between SEF and foramen ovale, foramen spinosum, and midline.(Fig. 3. A)

The presence of OC was examined on coronal sections and their laterality was recorded.(Fig. 3. B) Sphenoid sinus mucosa dimensions (SSMD) were categorized as less than 1 mm, 1-3 mm, or greater than 3 mm on sagittal and coronal sections.(Fig. 4) SSP was assessed on sagittal sections and classified as conchal, pre-sellar, sellar, or post-sellar.(Fig. 5)

### 3. Statistical analysis

All statistical analyses of the data were completed using IBM SPSS Statistics for Windows software (ver. 22.0; IBM, Armonk, NY, USA). Descriptive statistical methods (frequency, minimum, maximum, average, and standard deviation) were used for the data evaluation, and the chi-square test, Fisher-Freeman-Halton test, and continuity (Yates) correction were used to compare qualitative data. Significance was evaluated at the $P<0.05$ level.

## III. Results

The study included CBCT scans of 500 patients, comprising 292 females (58.4%) and 208 males (41.6%). The ages of the patients ranged from 7 to 89 years (mean, 36.32±17.89 years). Table 1 presents the age groups and sex distribution of the patients.

Table 2 presents the distribution, type, shape, laterality, and measurements for the cranial base anomalies.

An FNM was found in 26.0% of the 500 patients. The frequencies of SEF and CBM were 47.4% and 22.4%, respectively. Ninety-two of the detected sphenoid emissary foramina were unilateral, and 60 of these were on the right side and 32 were on the left side.

Table 3 presents the distribution of OC, SSMD, and SSP.

Of the 92 (18.4%) OC identified, 65 (70.7%) were unilateral; and of these, 31 were on the right side and 34 were on the left side.

An FNM, CBM, or OC was present in 28.1%, 19.5%, and 18.5% of females, and 23.1%, 26.4%, and 18.3% of males, respectively. No statistically significant relationships between


**Fig. 3.** A. Sphenoid emissary foramen and measurements (straight arrow: sphenoid emissary foramen, dashed arrow: foramen spinosum, arrowhead: foramen ovale; a: distance between sphenoid emissary foramen and midline, b: distance between sphenoid emissary foramen and foramen ovale, c: distance between sphenoid emissary foramen and foramen spinosum). B. Illustration of an Onodi cell (arrow).
*Aslıhan Akbulut et al: Investigation of the prevalence and main features of skull-base anomalies and characteristics of the sphenoid sinus using cone-beam computed tomography. J Korean Assoc Oral Maxillofac Surg 2022*

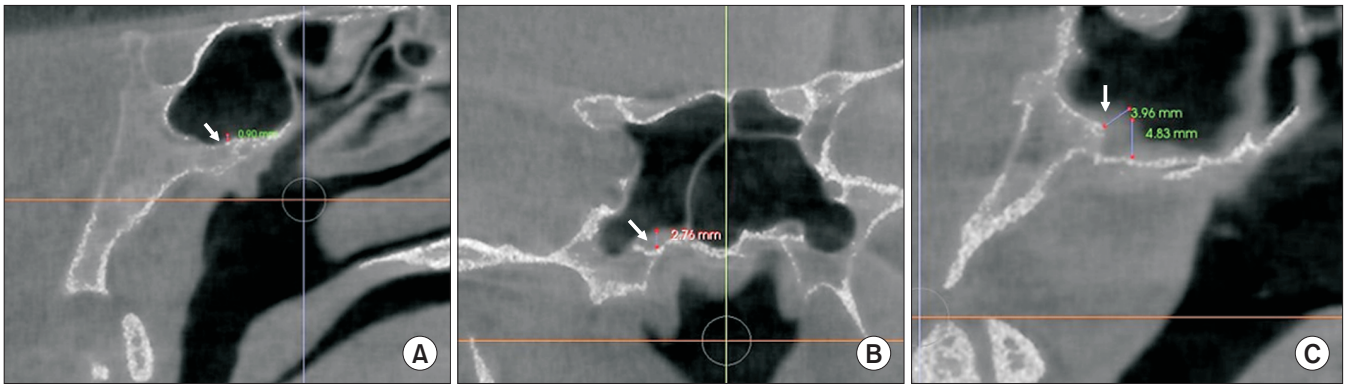


**Fig. 4.** Sphenoid sinus mucosa and measurements (arrows). A. Sphenoid sinus mucosa dimensions (SSMD) less than 1 mm. B. SSMD 1-3 mm. C. SSMD greater than 3 mm.
*Aslıhan Akbulut et al: Investigation of the prevalence and main features of skull-base anomalies and characteristics of the sphenoid sinus using cone-beam computed tomography. J Korean Assoc Oral Maxillofac Surg 2022*

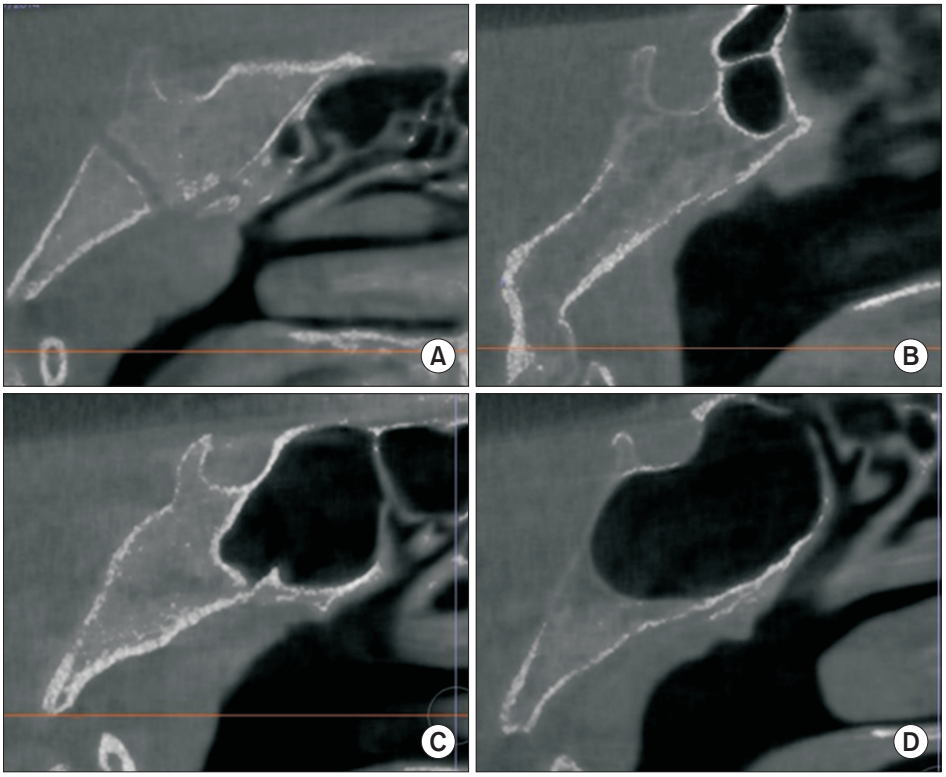


**Fig. 5.** Sphenoid sinus pneumatization. A. Conchal. B. Pre-sellar. C. Sellar. D. Post-sellar.
*Aslıhan Akbulut et al: Investigation of the prevalence and main features of skull-base anomalies and characteristics of the sphenoid sinus using cone-beam computed tomography. J Korean Assoc Oral Maxillofac Surg 2022*

**Table 1.** Distribution of the demographic data

| Characteristic | n (%) |
|---|---|
| Sex | |
| Male | 208 (41.6) |
| Female | 292 (58.4) |
| Age group | |
| <18 | 86 (17.2) |
| 18-29 | 112 (22.4) |
| 30-39 | 76 (15.2) |
| 40-49 | 94 (18.8) |
| 50-59 | 74 (14.8) |
| ≥60 | 58 (11.6) |

*Aslıhan Akbulut et al: Investigation of the prevalence and main features of skull-base anomalies and characteristics of the sphenoid sinus using cone-beam computed tomography. J Korean Assoc Oral Maxillofac Surg 2022*

FNM, CBM, or OC and sex were evident ($P$=0.209, $P$=0.067, $P$=0.949, respectively; $P$>0.05).

In female patients, 150 (51.4%) sellar-type, 117 (40.1%) post-sellar type, 17 (5.8%) pre-sellar type, and 8 (2.7%) conchal-type SSP were detected. Among male patients, 112 (53.8%) had sellar-type, 74 (35.6%) post-sellar type, 14 (6.7%) pre-sellar type, and 8 (3.8%) conchal-type SSP. With respect to SSP, no statistically significant difference between sexes was evident ($P$=0.703; $P$>0.05).

The percentage of patients with SEF was significantly higher in females (53.1%) than in males (39.4%, $P$=0.003; $P$<0.05).

Measurement of SSMD showed a statistically significant difference between sexes. The presence of a ">3 mm" mucosa was detected in a significantly greater percentage of male (n=57, 27.4%) than female (n=48, 16.4%) patients ($P$=0.012; $P$<0.05). Mucosa dimensions "≤1" mm and "1-3" mm were detected in 126 (43.2%) and 77 (37%) of female patients and 118 (40.4%) and 74 (35.6%) of male patients. No statistically significant difference between sexes was found for "≤1" mm and "1-3" mm mucosa dimensions ($P$>0.05).

The relationships between age groups and evaluated variables are presented in Table 4.

There were statistically significant differences between the age groups with respect to the presence of an FNM ($P$=0.000; $P$<0.05). An FNM was detected in a significantly greater percentage of the 18-29 age group patients then in the less than 18, 40-49, and 50-59 age groups ($P$=0.012, 0.000, and 0.001, respectively; $P$<0.05). In addition, FNM was detected in a greater percentage of patients in the 30-39 age group than in the 40-49 and 50-59 age groups ($P$=0.005 and 0.028, respectively; $P$<0.05) and in the greater than 60 age group than in the 40-49 age group ($P$=0.036; $P$<0.05).

There were also significant differences between the various age groups with respect to the presence of an SEF ($P$=0.002; $P$<0.05). In the greater than 60 age group, the percentage of patients with SEF was significantly lower than in the below 18, 18-29, 30-39, and 40-49 age groups ($P$=0.005, 0.000,

**Table 2.** Distribution, type, shape, laterality, and measurements of cranial-base anomalies

| | (+) | (–) |
|---|---|---|
| FNM | 130/500 (26.0) | 370/500 (74.0) |
| Dimension (mm) | | |
| Width | 4.47±1.61 (1.25-9.30) | |
| Length | 4.65±1.93 (1.36-9.12) | |
| Depth | 1.87±0.66 (0.73-4.09) | |
| SEF | 237/500 (47.4) | 263/500 (52.6) |
| Laterality | | |
| Unilateral | 70/237 (29.5) | |
| Bilateral | 167/237 (70.5) | |
| Type | | |
| Type 1 | 77/438 (17.6) | |
| Type 2 | 156/438 (35.6) | |
| Type 3 | 205/438 (46.8) | |
| Shape | | |
| Round | 307/438 (70.1) | |
| Oval | 109/438 (24.9) | |
| Irregular | 22/438 (5.0) | |
| Diameter (mm) | 1.07±0.50 (0.12-2.34) | |
| SEF-FO (mm) | 3.29±2.11 (0.36-21.39) | |
| SEF-FS (mm) | 12.44±2.85 (1.30-23.84) | |
| SEF-midline (mm) | 19.20±3.23 (3.09-29.87) | |
| CBM | 112/500 (22.4) | 388/500 (77.6) |
| Bifurcation | 4/112 (3.6) | |
| Inferior | 37/112 (33.0) | |
| Superior | 22/112 (19.6) | |
| Inferior recess | 38/112 (33.9) | |
| Superior recess | 5/112 (4.5) | |
| Channel | 6/112 (5.4) | |

(FNM: fossa navicularis magna, SEF: sphenoid emissary foramen, FO: foramen ovale, FS: foramen spinosum, CBM: canalis basilaris medianus)

Values are presented as number (%) or mean±standard deviation (range).

*Aslıhan Akbulut et al: Investigation of the prevalence and main features of skull-base anomalies and characteristics of the sphenoid sinus using cone-beam computed tomography. J Korean Assoc Oral Maxillofac Surg 2022*

**Table 3.** Onodi cells (OC), sphenoid sinus mucosa dimensions (SSMD), and sphenoid sinus pneumatization (SSP) pattern

| | Value |
|---|---|
| OC | |
| (+) | 92 (18.4) |
| (–) | 408 (81.6) |
| Unilateral | 65/92 (70.7) |
| Bilateral | 27/92 (29.3) |
| SSMD | |
| ≤1 mm | 203 (40.6) |
| 1-3 mm | 192 (38.4) |
| >3 mm | 105 (21.0) |
| SSP | |
| Conchal | 16 (3.2) |
| Pre-sellar | 31 (6.2) |
| Sellar | 262 (52.4) |
| Post-sellar | 191 (38.2) |

Values are presented as number (%).

*Aslıhan Akbulut et al: Investigation of the prevalence and main features of skull-base anomalies and characteristics of the sphenoid sinus using cone-beam computed tomography. J Korean Assoc Oral Maxillofac Surg 2022*

0.017, and 0.005, respectively; $P<0.05$). Similarly, in the 50-59 age group, the presence of an SEF was detected in a lower percentage of patients than in the 18-29 age group ($P=0.0196$; $P<0.05$).

Statistically, significant differences were noted between age groups in terms of the presence of SSMDs ($P=0.000$; $P<0.05$). Mucosal dimensions "greater than 3 mm" were measured in a significantly greater percentage of patients in the less than 18 age group than the 18-29, 30-39, 50-59, and the greater than 60 age groups ($P=0.00$, 0.015, 0.041, and 0.002, respectively; $P<0.05$). A "greater than 3 mm" mucosal measurement was recorded in a significant percentage of patients in the 40-49 age group compared to the 18-29 age group ($P=0.000$; $P<0.05$).

In terms of post-sellar SSP, in the less than 18 age group, the percentage of patient with this anomaly was lower than in the other age groups. *P*-values for all group comparions were less than 0.05.

Table 5 presents the relationships between the SSMD and the presence of a FNM, CBM, SEF, or OC. The interrelationships between the SSP pattern and the above-mentioned skull-base anomalies and OC are also provided.

No statistically significant relationship between the sinus mucosa and cranial base anomalies was identified, nor any correlations between the presence of OC and SSMD ($P>0.05$).

SSP was not related to cranial base anomalies or the presence of OC ($P>0.05$).

## IV. Discussion

Anomalies of the middle portion of the skull base, although relatively rare, should be considered in the radiological examinations before initiating any surgical procedures, or investigating possible infection or tumor spread pathways.

A FNM is a rare anomaly of the inferior aspect of the clivus and may be associated with spread of infection from the posterior pharynx to the base of the skull[18,19].

Murjani et al.[20] evaluated 350 CBCT scans for the presence of skull base anomalies and reported 19.4% of images had detectable FNM; they also reported no difference between sexes and age groups with respect to the occurrence of FNM. Akkoca Kaplan et al.[21], in their recent study, investigated the prevalence of FNM by evaluating the CBCT scans of 195 patients. They defined 32 (16.4%) FNM and found no correlation between FNM and sex or age group. According to their measurements, FNM depths ranged between 1.0 mm and 5.1 mm, lengths ranged between 1.0 mm to 8.9 mm, and widths ranged between 1.5 mm and 8.4 mm[21]. Another CBCT

**Table 4.** The relationships between age group and cranial-base anomalies, OC, SSMD, and SSP

| | Age group | | | | | | *P*-value |
|---|---|---|---|---|---|---|---|
| | <18 (n=86) | 18-29 (n=112) | 30-39 (n=76) | 40-49 (n=94) | 50-59 (n=74) | ≥60 (n=58) | |
| FNM | | | | | | | |
| (–) | 66 (76.7) | 67 (59.8) | 52 (68.4) | 81 (86.2) | 62 (83.8) | 42 (72.4) | 0.000* |
| (+) | 20 (23.3) | 45 (40.2) | 24 (31.6) | 13 (13.8) | 12 (16.2) | 16 (27.6) | |
| CBM | | | | | | | |
| (–) | 75 (87.2) | 86 (76.8) | 60 (78.9) | 66 (70.2) | 54 (73.0) | 47 (81.0) | 0.111 |
| (+) | 11 (12.8) | 26 (23.2) | 16 (21.1) | 28 (29.8) | 20 (27.0) | 11 (19.0) | |
| SEF | | | | | | | |
| (–) | 40 (46.5) | 47 (42.0) | 41 (53.9) | 48 (51.1) | 44 (59.5) | 43 (74.1) | 0.002* |
| (+) | 46 (53.5) | 65 (58.0) | 35 (46.1) | 46 (48.9) | 30 (40.5) | 15 (25.9) | |
| OC | | | | | | | |
| (–) | 73 (84.9) | 92 (82.1) | 59 (77.6) | 77 (81.9) | 58 (78.4) | 49 (84.5) | 0.810 |
| (+) | 13 (15.1) | 20 (17.9) | 17 (22.4) | 17 (18.1) | 16 (21.6) | 9 (15.5) | |
| SSMD | | | | | | | |
| ≤1 mm | 21 (24.4) | 62 (55.4) | 30 (39.5) | 27 (28.7) | 32 (43.2) | 31 (53.4) | 0.000* |
| 1-3 mm | 38 (44.2) | 37 (33.0) | 29 (38.2) | 43 (45.7) | 25 (33.8) | 20 (34.5) | |
| >3mm | 27 (31.4) | 13 (11.6) | 17 (22.4) | 24 (25.5) | 17 (23.0) | 7 (12.1) | |
| SSP | | | | | | | |
| Conchal | 7 (8.1) | 5 (4.5) | 1 (1.3) | 0 (0) | 3 (4.1) | 0 (0) | 0.000* |
| Pre-sellar | 8 (9.3) | 6 (5.4) | 5 (6.6) | 3 (3.2) | 4 (5.4) | 5 (8.6) | |
| Sellar | 56 (65.1) | 51 (45.5) | 33 (43.4) | 50 (53.2) | 38 (51.4) | 34 (58.6) | |
| Post-sellar | 15 (17.4) | 50 (44.6) | 37 (48.7) | 41 (43.6) | 29 (39.2) | 19 (32.8) | |

(OC: Onodi cells, SSMD: sphenoid sinus mucosa dimensions, SSP: sphenoid sinus pneumatization, FNM: fossa navicularis magna, CBM: canalis basilaris medianus, SEF: sphenoid emissary foramen)
*$P$<0.05 by chi-square test.
Values are presented as number (%).
*Aslıhan Akbulut et al: Investigation of the prevalence and main features of skull-base anomalies and characteristics of the sphenoid sinus using cone-beam computed tomography. J Korean Assoc Oral Maxillofac Surg 2022*

**Table 5.** SSMDs, SSP, OC, and cranial-base anomalies

| | SSMD | | | | SSP | | | | |
|---|---|---|---|---|---|---|---|---|---|
| | ≤1 mm (n=203) | 1-3 mm (n=192) | >3 mm | *P*-value | Conchal (n=16) | Pre-sellar (n=31) | Sellar (n=262) | Post-sellar (n=191) | *P*-value |
| FNM | | | | | | | | | |
| (–) | 151 (74.4) | 139 (72.4) | 80 (76.2) | 0.766[1] | 13 (81.3) | 24 (77.4) | 205 (78.2) | 128 (67.5) | 0.053[1] |
| (+) | 52 (25.6) | 53 (27.6) | 25 (23.8) | | 3 (18.8) | 7 (22.6) | 57 (21.8) | 63 (33.0) | |
| CBM | | | | | | | | | |
| (–) | 161 (79.3) | 145 (75.5) | 82 (78.1) | 0.659[1] | 14 (87.5) | 25 (80.6) | 206 (78.6) | 143 (74.9) | 0.626[1] |
| (+) | 42 (20.7) | 47 (24.5) | 23 (21.9) | | 2 (12.5) | 6 (19.4) | 56 (21.4) | 48 (25.1) | |
| SEF | | | | | | | | | |
| (–) | 103 (50.7) | 107 (55.7) | 53 (50.5) | 0.542[2] | 9 (56.3) | 19 (61.3) | 129 (49.2) | 106 (55.5) | 0.414[2] |
| (+) | 100 (49.3) | 85 (44.3) | 52 (49.5) | | 7 (43.8) | 12 (38.7) | 133 (50.8) | 85 (44.5) | |
| OC | | | | | | | | | |
| (–) | 170 (83.7) | 152 (79.2) | 86 (81.9) | 0.500[1] | 15 (93.8) | 29 (93.5) | 207 (79.0) | 157 (82.2) | 0.135[1] |
| (+) | 33 (16.3) | 40 (20.8) | 19 (18.1) | | 1 (6.3) | 2 (6.5) | 55 (21.0) | 34 (17.8) | |

(SSMD: sphenoid sinus mucosa dimensions, SSP: sphenoid sinus pneumatization, OC: Onodi cells, FNM: fossa navicularis magna, CBM: canalis basilaris medianus, SEF: sphenoid emissary foramen)
[1]Fisher-Freeman-Halton test, [2]chi-square test.
Values are presented as number (%).
*Aslıhan Akbulut et al: Investigation of the prevalence and main features of skull-base anomalies and characteristics of the sphenoid sinus using cone-beam computed tomography. J Korean Assoc Oral Maxillofac Surg 2022*

study of 168 patients found an FNM prevalence of 27.5%. The average depth, length, and width were 2.22 mm, 8.5 mm, and 5.37 mm, respectively. No sex predisposition for the presence of an FNM was reported; however, a positive correlation between patient age and length of the FNM was noted[22]. In a more extensive study of 723 CBCT scans, the prevalence of FNM was 6.6% and a predominance among males was reported. The average depth of FNM was 2.2 mm, the length was 5.8 mm and the width was 4.7 mm[15]. Bayrak et al.[7] examined computed tomography (CT) and CBCT scans of 1,059 patients and found an FNM in 81 (7.6%) of them. They found an average FNM depth of FNM 2.76 mm and 4.17 mm, aver-

age length of 7.15 mm and 4.12 mm, and average width of 5.23 mm and 4.08 mm on CBCT and CT scans, respectively. They also reported that the length of FNM was significantly higher in males and the length of FNM was lower in 30-39 age group compared to 10-19, 40-49, and >50 age groups[7].

In our study, the prevalence of FNM in the 500 patients that formed our study group was 26.0%. The FNM width was 4.47±1.61 mm, the length was 4.65±1.93 mm, and the depth was 1.87±0.66 mm. We found no correlation between sex and the presence of FNM, but there were significant differences between the age groups: FNM was more frequent in the 18-29 age group (40.2%) than in the 40-49, 50-59, and less than 18 age groups. Also, FNM was detected in a greater percentage of the 30-39 age group than of the 40-49 and 50-59 age groups, and the greater than 60 age group showed higher values compared to the 40-49 age group. In terms of FNM frequency, while our results are compatible with some of the above-mentioned studies[20,22], some inconsistencies are evident[6,7,21]. The lack of consistency among the vairous studies may be related to methodologic differences, sample size and properties of the samples (patients). In this study, there was no effect of sex on the detection of FNM, and this finding is similar to those of most previous reports, except for one study in which FNM was identified in a greater proportion of males than females[15]. The FNM dimensions measured in this study were comparable to those from previous reports.

When defining an FNM, an important question should be: "Is that radiolucent, well-defined structure in the inferior part of the clivus a FNM or a CBM (inferior recess type)?" Some researchers consider an FNM to be a sub-type of CBM[14]. In our study we made the distinction between these two anatomic variations according to adiographic appearance and dimensions. If the depth of the radiolucent structure did not extend beyond the mediolateral (width) and inferosuperior (length) dimensions, the structure was considered a "fossa."

Although a CBM is a rare anomaly, with a prevalence between 2% and 5.5%[4,5,23,24], a CBM may be found incidentally on radiographic examinations or may sometimes be symptomatic and associated with meningitis and cerebrospinal fluid leak[5,23,24]. It is important to properly identify these anomalies.

Several recent studies have used CBCT to define the prevalence and characteristics of CBM. Akkoca Kaplan et al.[6], in their CBCT study of 350 patients, identified CBM in 15 (4.3%). No sex correlation was observed; however, the anomaly was significantly more common in the 6-15 age group than in the 22-30 age group[6]. In another study of CT and CBCT scans from 1,059 patients, CBM prevalence was 2.5% (26 patients). They reported no influence of sex on CBM detection and no correlation with patient age. Types 1, 3, and 5 CBM were found in seven patients each, Type 4 was found in 3 patients, and Types 2 and 6 were found in one patient[7]. Another CT study that included 350 patients defined the prevalence of CBM as 9.7%. No difference between female and male patients was found and the anomaly was not associated with patient age. In terms of types of CBM; no bifurcation-type (Type 1) CBM was identified and the most common types were inferior and superior recess (Types 4 and 5). Incomplete types were detected more frequently than complete types[20].

Compared to previous reports, this study found a higher percentage (22.4%) of CBM anomalies. This difference may be related to the sample size and properties, and methodologic differences, especially the exclusion criteria defined by the researchers. Artifacts on CBCT scans may interfere with optimal analysis of the images and may lead to some anomalies—especially with sub-millimeter dimensions—being overlooked. The inferior recess type (Type 4) of CBM was the most frequent type in this study. In contrast, this type of CBM was the second most common in Murjani et al.[20] and fourth most common in Bayrak et al.[7]. Sex and age features were comparable with those of previous studies[7,20].

A SEF (also known as foramen of Vesalius) is a connection between the cavernous sinus and pterygoid plexus located in the greater wing of the sphenoid bone. The foramen contains a small vein that provides drainage of the cavernous sinus[16,25]. Numerous studies have investigated the prevalence and characteristic features of this bony canal. Poornima et al.[26] evaluated 100 skulls for the presence of SEF, and they found 34 bilateral and 26 unilateral SEF in 60 skulls. Of the unilateral SEF, 15 were on the right side and 11 were on the left side[26]. Another study of 150 skulls reported 29 bilateral and 32 unilateral SEF. Forty-one of the SEF were on the right side and 49 were on the left side. In the same study of the identified 90 SEF, 64 (72%), 22 (24%), and 4 (4%) were defined as round, oval, and irregularly shaped, respectively. The average diameter of this foramen was 0.98 mm on the right side and 1.12 mm on the left side[27]. Pathmashri and Thenmozi[28] studied 50 skulls and found 6 (12%) had bilateral SEF and no unilateral SEF. They reported that four skulls had round-shaped and two had oval-shaped SEF, and the diameter of the SEF ranged from 1 to 2 mm[28]. Ozer and Govsa[25] analyzed 172 cranial bases for the presence of SEF and found SEF in 60 (34.8%) of the specimens and 16 of them were bilateral; of

the 44 unilateral SEF, 26 were on the left side and 18 were on the right side. They also classified the SEF according to the diameter as follows: Type 1, less than 0.5 mm; Type 2, 0.5 to 1 mm, and Type 3, greater than 1 mm. Type 1 SEF was found in 5 (8.3%) specimens and the incidence of Type 3 was 18.3%. The average distance between the SEF and the FO was 2.30 mm on the right side and 2.46 mm on the left side. The average distance between the SEF and the FS was 10.76 mm and 10.42 mm on the right and left sides, respectively[25]. Leonel et al.[29] studied 1,000 CT images and 170 skulls to determine the prevalence and characteristics of SEF. They found that 468 (46.8%) of the 1,000 CT scans showed SEF, 25.4% were bilateral, and 21.4% were unilateral. Seventy-seven (43.2%) skulls showed SEF; of these, 32 (18.8%) were bilateral and 45 (26.4%) (25 left, 20 right) were unilateral[29]. Akkoca Kaplan et al.[6] investigated 350 CBCT scans retrospectively and reported 145 (41.1%) had detectable SEF. Bayrak et al.[30] studied 317 CBCT scans and found an SEF in 89 (28.1%) of the study images with no differences between sexes; 76 (21.1%) were unilateral and 22 (6.9%) were bilateral. The average diameter of the SEF was 2.66 mm on the right side and 2.82 mm on the left side. The diameter of SEF did not differ between the sexes. The average SEF-FO distance was 2.31 mm and 2.21 mm, SEF-FS distance was 11.32 mm and 11.26 mm, SEF-midline distance was 19.57 mm and 15.8 mm on the right and left sides, respectively. Of the foramina detected, 28 (25.2%) were round, 76 (68.5%) were oval, and 7 (6.3%) were irregular in shape[30].

In our study group, the SEF frequency was 47.4%. While our results are consistent with the finding of previous studies[6,26,27,29], some reported lower frequencies of SEF detection[25,30]. This may be a result of the difference between study groups, study method, and, especially in radiographic studies, the exclusion criteria. Bilateral SEF was more frequent in our study, similar to the findings of Poornima et al.[26] and Leonel et al.[29]. In this study, the incidence of SEF in females (53.1%) was significantly greater than that of males (39.4%). Also, significant differences between age groups were observed in our study. The incidence of SEF in patients over the age of 60 was significantly lower than in the less than 18, 18-29, 30-39, and 40-49 age groups, and the incidence of SEF in the 50-59 age group was significantly lower than in the 18-29 age group. The finding of lower SEF incidence in the older age groups may represent sclerosis of the foramen with age; however, this hypothesis has no supporting data at this time. Type 3 SEF was the most common type identified in our study, followed by Types 2 and 1. This type of classification was solely made by Ozer and Govsa[25]; however, they reported Type 2 SEF as the most frequent type, followed by Types 3 and 1. In this study, average SEF diameter was 1.07 mm. Raval et al.[27] reported similar measurements, while Bayrak et al.[30] reported higher values. This difference may have been the result of the exclusion criteria applied, which may affect the visibility of these small and sometimes sub-millimeter structures. The average SEF-FO distance was 3.29 mm, the SEF-FS distance was 12.44 mm and SEF-midline distance was 19.20 mm in our study, which are comparable to the results reported by Bayrak et al.[30] and Ozer and Govsa[25]. The majority of the SEFs detected in our study was round, consistent with some previous reports[27,28]; however, Bayrak et al.[30] found that oval-shaped SEF were more frequently identified.

OCs are the most posterior ethmoid air cells and may project into the sphenoid sinus, leading to problems during transsphenoidal pituitary surgeries; in addition, their proximity to some vital structures, such as the optic canal and internal carotid artery, may result in damage to these structures during sinus surgery[11,12,31,32]. Thus, identification of these anomalous air cells is necessary prior to any surgical procedure involving the sphenoid sinus and surrounding structures.

Thimmaiah and Anupama[12] retrospectively investigated 1,080 CT scans and found 260 (24.07%) OCs, 163 (62.69%) in males and 97 (37.31%) in females. Badawi et al.[32] evaluated 61 CT scans and found OCs in 18 (29.5%) patients. Bilateral OC was detected in 7 (11.5%) patients, and unilateral OC were detected in 11 (18%) patients. Of the evaluated females and patients, 75% and 65.5% showed no OC, respectively[32]. Wada et al.[33] analyzed 261 CT scans of chronic rhinosinusitis patients and found OCs in 50.8%. Another CT study of 450 patients reported 65 (14.4%) had OC, and the vast majority of the identified OC was unilateral. Although not significant, females tended to have more OC than the male patients[34]. A more comprehensive study of 618 CT scans of patients with sinonasal symptoms reported OC in 326 (52.7%); 154 (47.3%) of who showed bilateral cells. The relationship between sphenoiditis and OCs was also investigated. Sphenoiditis was defined as sphenoid sinus mucosa greater than 2 mm and was identified in 121 (19.6%) patients. Sphenoiditis was significantly more common in males, while OC were 1.5 times more frequent in patients with sphenoiditis[35]. Ali et al.[11] evaluated 201 CBCT scans for the presence of OC and reported finding them in 86 (42.8%) scans, with no differences between the sexes. Shokri et al.'s analysis[36] of 250 CBCT scans for the presence of OC resulted in a frequency of 37.2%, no sex predominance, and no differences between

age groups.

In our study, OC were identified in 18.4% of patients and more than two-thirds of the OC identified were unilateral. No difference between sexes and age groups was identified in terms of OC presence. As summarized above, there are discrepancies between studies that have investigated the prevalence of OC, and these may be a result of differences between study groups, study methods, and assessment criteria. Most studies have shown that OC are more frequently unilateral, with no differences between males and females, as in our study.

SSP may be assessed according to the sinus volume, the relative position with respect to the sella turcica, and extension of pneumatization to parts of sphenoid bone (anterior clinoid process, pterygoid process, etc.). On sagittal sections, the sphenoid sinus position relative to the sella turcica can be classified as conchal, pre-sellar, sellar, or post-sellar[3].

In their retrospective CT and magnetic resonance imaging (MRI) study, Hamid et al.[9] investigated SSP in patients with pituitary adenomas. The study included 296 patients, of which 6 (2%), 62 (21%), 162 (54.7%), and 66 (22.3%) were identified as having conchal, pre-sellar, sellar, or post-sellar pneumatization, respectively[9]. Five hundred CT scans were evaluated by Hiremath et al.[10] and showed no conchal-type pneumatization, although six (1.2%) patients had pre-sellar, 111 (22.2%) had incomplete sellar, and 383 (76.6%) had complete sellar pneumatization. They reported no significant difference between sexes in terms of SSP[10]. In their study of 60 CT scans, Idowu et al.[37] reported 0% conchal pneumatization, 3 (5%) pre-sellar, 53 (83%) sellar, and 4 (6.7%) post-sellar pneumatization. Another CT study reported 11.2% pre-sellar-type, 14% sellar-type, and 74.8% post-sellar-type SSP[38].

In our study, the numbers and percentages of patients with conchal-, pre-sellar-, sellar- and post-sellar-type SSP were 16 (3.2%), 31 (6.2%), 262 (52.4%), and 191 (38.2%), respectively. No significant difference between sexes were noted. Sellar-type pneumatization was the most common, followed by the post-sellar type. These results were consistent with some, but not all previous reports[9,10,37,38]. Inconsistencies between the studies may be the consequence of varying age ranges. Our study group had a relatively lower average age, and the youngest patient was 6 years old, while most other studies were conducted in older age groups. Sphenoid pneumatization reaches the adult size sometime between 10 and 18 years of age, and pneumatization of the sphenoid sinus progresses toward the inferior, posterolateral direction after its onset[3]. Another finding of our study that supports the above-mentioned developmental properties was that the frequency of the post-sellar type was significantly lower in patients less than 18 years of age than in the other age groups.

The radiographic appearance of the inner structure of the sphenoid sinus may show alterations for various reasons. For example, inflammation, tumors, or less common pathologies such as cerebrospinal fluid leakage, meningocele, meningoencephalocele, and vascular lesions may be present[39]. Fooanant et al.[39] investigated CT and MRI findings, endoscopy results, clinical symptom records, and microbiologic and pathological reports of 122 patients retrospectively; about 80% of the lesions they discovered had inflammatory origins and about 20% had tumor origins. The vast majority of the inflammatory lesions were bacterial and fungal[39]. Kanwar et al.[40] investigated 91 patients with chronic rhinosinusitis symptoms using CT and histopathologic examinations. Histopathologic examination of the lesions indicated 57.2% of patients had non-specific inflammation, and the sphenoid sinus was the least commonly involved sinus[40]. Marcolini et al.[41] studied 46 patients with isolated sphenoid sinus pathologies and found that 12 (26.1%) had isolated sphenoiditis, while 22 (47.8%) had mucoceles, 3 (6.5%) had fungal sphenoiditis, 3 (6.5%) had sphenochoanal polyps, 2 (4.3%) had cerebrospinal fluid leak, and 1 (2.1%) each had meningoencephalocele, inverted papilloma, fibrous dysplasia, or squamous cell carcinoma[41]. Turgut et al.[42] examined CT scans of 221 patients and found that 24 had sphenoid sinus involvement. Eight patients had isolated sphenoid sinus disease[42]. Almomen et al.[43] included 30 patients with isolated sphenoid sinus disease, and the most common pathology was bacterial sphenoid sinusitis, followed by a fungal ball. Kushwah et al.[44] retrospectively analyzed 50 patients with paranasal sinus diseases using CT and histopathologic reports. The most commonly affected sinus was the maxillary sinus, followed by sphenoid, ethmoid, and frontal sinuses. Paranasal sinus diseases were more frequent in males, and non-specific inflammation was the most common diagnosis[44].

In this study, 203 (40.6%) patients showed had mucosa less than 1 mm in thickness, 192 (38.4%) showed mucosa 1-3 mm, and 105 (21.0%) presented greater than 3 mm. The presence of sphenoid sinus mucosa greater than 3 mm was more common in males. In addition, patients less than 18 years of age had significantly greater percentages of patients with greater than 3 mm sphenoid sinus mucosa. One of the limitations of this study was that there was no opportunity to make a distinction between sinus pathologies or to assess the clini-

cal symptoms of the patients included in the study because of the retrospective and radiographic nature. Although CBCT is considered superior for examinations of hard tissues, it is considered a poor method to use when imaging soft tissues and making a radiographic diagnosis of the pathologies of the soft tissues.

The dimensions of the sphenoid sinus mucosa and SSP showed no correlation with the presence of FNM, CBM, SEF, or OC in this study.

## V. Conclusion

The base of the skull and the sphenoid sinus are anatomical structures that may be found in the field of view of CBCT scans. Anomalies of the skull base are common findings that may be identified incidentally during CBCT investigations performed for various reasons; however, alterations in the dimensions of the sphenoid sinus or sphenoid sinus mucosa and the existence of OC are of clinical importance. Regardless of the reason for CBCT investigations, it is important to define and report these anatomical structures and variations.

## ORCID

Aslıhan Akbulut, *https://orcid.org/0000-0001-7931-4464*
Oğuzhan Demirel, *https://orcid.org/0000-0002-4756-6496*
Kaan Orhan, *https://orcid.org/0000-0001-6768-0176*

## Authors' Contributions

A.A. participated in the study design, data collection and data analysis. O.D. participated in data analysis, wrote the manuscript and helped to draft the manuscript. K.O. participated in the study design, coordination and wrote the manuscript.

## Ethics Approval and Consent to Participate

Ethical approval of the study was obtained from the ethics committee of İstanbul Medipol University, Clinical Research Ethics Committee (No. 10840098-772.02-E.34484). The written informed consent was obtained from all patients.

## Conflict of Interest

No potential conflict of interest relevant to this article was reported.

## References

1. Policeni BA, Smoker WR. Imaging of the skull base: anatomy and pathology. Radiol Clin North Am 2015;53:1-14. https://doi.org/10.1016/j.rcl.2014.09.005
2. Rai R, Iwanaga J, Shokouhi G, Loukas M, Mortazavi MM, Oskouian RJ, et al. A comprehensive review of the clivus: anatomy, embryology, variants, pathology, and surgical approaches. Childs Nerv Syst 2018;34:1451-8. https://doi.org/10.1007/s00381-018-3875-x
3. Cellina M, Gibelli D, Floridi C, Toluian T, Valenti Pittino C, Martinenghi C, et al. Sphenoid sinuses: pneumatisation and anatomical variants-what the radiologist needs to know and report to avoid intraoperative complications. Surg Radiol Anat 2020;42:1013-24. https://doi.org/10.1007/s00276-020-02490-y
4. Syed AZ, Zahedpasha S, Rathore SA, Mupparapu M. Evaluation of canalis basilaris medianus using cone-beam computed tomography. Imaging Sci Dent 2016;46:141-4. https://doi.org/10.5624/isd.2016.46.2.141
5. Currarino G. Canalis basilaris medianus and related defects of the basiocciput. AJNR Am J Neuroradiol 1988;9:208-11.
6. Akkoca Kaplan F, Bayrakdar İŞ, Bilgir E. Incidence of anomalous canals in the base of the skull: a retrospective radio-anatomical study using cone-beam computed tomography. Surg Radiol Anat 2020;42:171-7. https://doi.org/10.1007/s00276-019-02307-7
7. Bayrak S, Göller Bulut D, Orhan K. Prevalence of anatomical variants in the clivus: fossa navicularis magna, canalis basilaris medianus, and craniopharyngeal canal. Surg Radiol Anat 2019;41:477-83. https://doi.org/10.1007/s00276-019-02200-3
8. Kazkayasi M, Karadeniz Y, Altinok D, Koç C. [Investigation of the anatomic variations of the sphenoid sinus with the computed tomography]. KBB ve BBC Dergisi 2001;9:74-7. Turkish.
9. Hamid O, El Fiky L, Hassan O, Kotb A, El Fiky S. Anatomic variations of the sphenoid sinus and their impact on trans-sphenoid pituitary surgery. Skull Base 2008;18:9-15. https://doi.org/10.1055/s-2007-992764
10. Hiremath SB, Gautam AA, Sheeja K, Benjamin G. Assessment of variations in sphenoid sinus pneumatization in Indian population: a multidetector computed tomography study. Indian J Radiol Imaging 2018;28:273-9. https://doi.org/10.4103/ijri.IJRI_70_18
11. Ali IK, Sansare K, Karjodkar F, Saalim M. Imaging analysis of onodi cells on cone-beam computed tomography. Int Arch Otorhinolaryngol 2020;24:e319-22. https://doi.org/10.1055/s-0039-1698779
12. Thimmaiah VT, Anupama C. Pneumatization patterns of onodi cell on multidetector computed tomography. J Oral Maxillofac Radiol 2017;5:63-6. https://doi.org/10.4103/jomr.jomr_3_17
13. Beltramello A, Puppini G, El-Dalati G, Girelli M, Cerini R, Sbarbati A, et al. Fossa navicularis magna. AJNR Am J Neuroradiol 1998;19:1796-8.
14. Syed AZ, Mupparapu M. Fossa navicularis magna detection on cone-beam computed tomography. Imaging Sci Dent 2016;46:47-51. https://doi.org/10.5624/isd.2016.46.1.47
15. Ersan N. Prevalence and morphometric features of fossa navicularis on cone beam computed tomography in Turkish population. Folia Morphol (Warsz) 2017;76:715-9. https://doi.org/10.5603/FM.a2017.0030
16. Shapiro R, Robinson F. The foramina of the middle fossa: a phylogenetic, anatomic and pathologic study. Am J Roentgenol Radium Ther Nucl Med 1967;101:779-94. https://doi.org/10.2214/ajr.101.4.779
17. Ónodi A. The optic nerve and the accessory sinuses of the nose: a contribution to the study of canalicular neuritis and atrophy of the optic nerve of nasal origin. New York (NY): William Wood; 1910.
18. Segal N, Atamne E, Shelef I, Zamir S, Landau D. Intracranial infection caused by spreading through the fossa naviclaris magna - a case report and review of the literature. Int J Pediatr Otorhinolaryn-

gol 2013;77:1919-21. https://doi.org/10.1016/j.ijporl.2013.09.013
19. Prabhu SP, Zinkus T, Cheng AG, Rahbar R. Clival osteomyelitis resulting from spread of infection through the fossa navicularis magna in a child. Pediatr Radiol 2009;39:995-8. https://doi.org/10.1007/s00247-009-1283-9
20. Murjani B, Bhosale R, Ramaswami E, Kadam S, Ramchandani A. Anatomical variations of clivus: a descriptive anatomical study. Surg Radiol Anat 2021;43:945-51. https://doi.org/10.1007/s00276-021-02686-w
21. Akkoca Kaplan F, Yesilova E, Bayrakdar IS, Ugurlu M. Evaluation of the relationship between age and gender of fossa navicularis magna with cone-beam computed tomography in orthodontic subpopulation. J Anat Soc India 2019;68:201-4.
22. Magat G. Evaluation of morphometric features of fossa navicularis using cone-beam computed tomography in a Turkish subpopulation. Imaging Sci Dent 2019;49:209-12. https://doi.org/10.5624/isd.2019.49.3.209
23. Jacquemin C, Bosley TM, al Saleh M, Mullaney P. Canalis basilaris medianus: MRI. Neuroradiology 2000;42:121-3. https://doi.org/10.1007/s002340050029
24. Khairy S, Almubarak AO, Aloraidi A, Alahmadi KOA. Canalis basalis medianus with cerebrospinal fluid leak: rare presentation and literature review. Br J Neurosurg 2019;33:432-3. https://doi.org/10.1080/02688697.2017.1346173
25. Ozer MA, Govsa F. Measurement accuracy of foramen of vesalius for safe percutaneous techniques using computer-assisted three-dimensional landmarks. Surg Radiol Anat 2014;36:147-54. https://doi.org/10.1007/s00276-013-1148-7
26. Poornima B, Phaniraj S, Mallikarjun M. A study of incidence of emissary sphenoidal foramen in dry adult human skull bones. Indian J Pharm Sci Res 2015;5:273-5.
27. Raval BB, Singh PR, Rajguru J. A morphologic and morphometric study of foramen vesalius in dry adult human skulls of gujarat region. J Clin Diagn Res 2015;9:AC04-7. https://doi.org/10.7860/JCDR/2015/11632.5553
28. Pathmashri VP, Thenmozhi D. Occurrence, shape and size of foramen vesalius in dry human skulls. J Pharm Sci Res 2015;7:718-9.
29. Leonel LCPC, Peris-Celda M, de Sousa SDG, Haetinger RG, Liberti EA. The sphenoidal emissary foramen and the emissary vein: anatomy and clinical relevance. Clin Anat 2020;33:767-81. https://doi.org/10.1002/ca.23504
30. Bayrak S, Kurşun-Çakmak EŞ, Atakan C, Orhan K. Anatomic study on sphenoidal emissary foramen by using cone-beam computed tomography. J Craniofac Surg 2018;29:e477-80. https://doi.org/10.1097/SCS.0000000000004492
31. Meybodi AT, Vigo V, Benet A. The Onodi cell: an anatomic illustration. World Neurosurg 2017;103:950.e5-6. https://doi.org/10.1016/j.wneu.2017.05.012
32. Badawi K, Madani GA, Seddeg Y. The radiological study of Onodi cells among adult sudanese subjects. IOSR-JDMS 2017;16:106-9.
33. Wada K, Moriyama H, Edamatsu H, Hama T, Arai C, Kojima H, et al. Identification of Onodi cell and new classification of sphenoid sinus for endoscopic sinus surgery. Int Forum Allergy Rhinol 2015;5:1068-76. https://doi.org/10.1002/alr.21567
34. Banaz F, Alnoury IS, Al-Shehri A, Alandejani T. Retrospective computed tomography prevalence of Onodi cells among adults in Jeddah, Saudi Arabia: age and gender difference. Am J Res Commun 2014;2:45-56.
35. Senturk M, Guler I, Azgin I, Sakarya EU, Ovet G, Alatas N, et al. The role of Onodi cells in sphenoiditis: results of multiplanar reconstruction of computed tomography scanning. Braz J Otorhinolaryngol 2017;83:88-93. https://doi.org/10.1016/j.bjorl.2016.01.011
36. Shokri A, Faradmal MJ, Hekmat B. Correlations between anatomical variations of the nasal cavity and ethmoidal sinuses on cone-beam computed tomography scans. Imaging Sci Dent 2019;49:103-13. https://doi.org/10.5624/isd.2019.49.2.103
37. Idowu OE, Balogun BO, Okoli CA. Dimensions, septation, and pattern of pneumatization of the sphenoidal sinus. Folia Morphol (Warsz) 2009;68:228-32.
38. Treviño-Gonzalez JL, Maldonado-Chapa F, Becerra-Jimenez JA, Soto-Galindo GA, Morales-Del Angel JA. Sphenoid sinus: pneumatization and septation patterns in a hispanic population. ORL J Otorhinolaryngol Relat Spec 2021;83:362-71. https://doi.org/10.1159/000514458
39. Fooanant S, Angkurawaranon S, Angkurawaranon C, Roongrotwattanasiri K, Chaiyasate S. Sphenoid sinus diseases: a review of 1,442 patients. Int J Otolaryngol 2017;2017:9650910. https://doi.org/10.1155/2017/9650910
40. Kanwar SS, Mital M, Gupta PK, Saran S, Parashar N, Singh A. Evaluation of paranasal sinus diseases by computed tomography and its histopathological correlation. J Oral Maxillofac Radiol 2017;5:46-52.
41. Marcolini TR, Safraider MC, Socher JA, Lucena GO. Differential diagnosis and treatment of isolated pathologies of the sphenoid sinus: retrospective study of 46 cases. Int Arch Otorhinolaryngol 2015;19:124-9. https://doi.org/10.1055/s-0034-1397337
42. Turgut S, Ozcan KM, Celikkanat S, Ozdem C. Isolated sphenoid sinusitis. Rhinology 1997;35:132-5.
43. Almomen A, Alshakhs A, Alturaifi A. The different causes and management of chronic sphenoid rhinosinusitis. Glob J Otolaryngol 2020;22:GJO.MS.ID.556076. https://doi.org/10.19080/GJO.2020.22.556076
44. Kushwah APS, Bhalse R, Pande S. CT evaluation of diseases of Paranasal sinuses & histopathological studies. Int J Med Res Rev 2015;3:1306-10. https://doi.org/10.17511/ijmrr.2015.i11.237

**How to cite this article:** Akbulut A, Demirel O, Orhan K. Investigation of the prevalence and main features of skull-base anomalies and characteristics of the sphenoid sinus using cone-beam computed tomography. J Korean Assoc Oral Maxillofac Surg 2022;48:207-218. https://doi.org/10.5125/jkaoms.2022.48.4.207